JACS Au
AN OPEN ACCESS JOURNAL OF THE AMERICAN CHEMICAL SOCIETY

pubs.acs.org/jacsau

Letter

Plasma-Induced Selective Propylene Epoxidation Using Water as the Oxygen Source

Dongho Lee, Han-Ting Chen, and Suljo Linic*

Cite This: *JACS Au* 2023, 3, 997−1003

Read Online

ACCESS | Metrics & More | Article Recommendations | Supporting Information

ABSTRACT: Propylene oxide (PO) is a critical gateway chemical used in large-scale production of plastics and many other compounds. In addition, PO is also used in many smaller-scale applications that require lower PO concentrations and volumes. These include its usage as a fumigant and disinfectant for food, a sterilizer for medical equipment, as well as in producing modified food such as starch and alginate. While PO is currently mostly produced in a large-scale propylene epoxidation chemical process, due to its toxic nature and high transport and storage costs, there is a strong incentive to develop PO production strategies that are well-suited for smaller-scale on-site applications. In this contribution, we designed a plasma−liquid interaction (PLI) catalytic process that uses only water and C_3H_6 as reactants to form PO. We show that hydrogen peroxide (H_2O_2) generated in the interactions of water with plasma serves as a critical oxidizing agent that can epoxidize C_3H_6 over a titanium silicate-1 (TS-1) catalyst dispersed in a water solution with a carbon-based selectivity of more than 98%. As the activity of this plasma C_3H_6 epoxidation system is limited by the rate of H_2O_2 production, strategies to improve H_2O_2 production were also investigated.

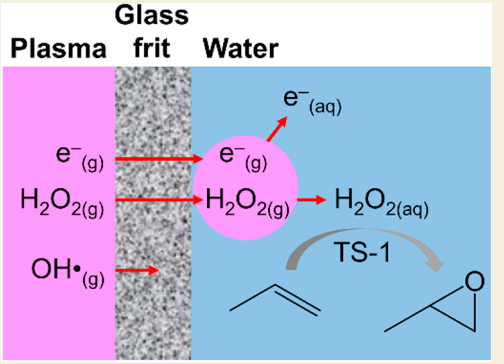

KEYWORDS: *plasma chemistry, plasma−liquid interaction, propylene epoxidation, decentralized chemical production, sustainable synthesis, hydrogen peroxide production*

Propylene oxide (PO) is an important feedstock chemical for production of various higher value chemicals and materials.[1,2] Conventional production of PO employs the chlorohydrin process, which generates chlorine salt byproducts and has a significant environmental footprint. Direct propylene (C_3H_6) epoxidation using oxygen (O_2) is a more desirable pathway to PO. The direct process, however, has been elusive.[3−5] An alternative C_3H_6 epoxidation approach employs hydrogen peroxide (H_2O_2) as an oxidizing agent. H_2O_2 is formed from O_2 and hydrogen (H_2). Though the hydrogen peroxide propylene epoxidation (HPPO) process generates water as the only byproduct and exhibits high PO selectivity,[2] the production of H_2O_2 relies on the energy-intensive and environmentally challenging anthraquinone process, which requires large-scale and centralized operation.[6] While the integration of the centralized H_2O_2 production and HPPO process has its advantage in large-scale industrial production of PO, there is also a significant need to develop chemical systems that can generate PO on demand and at smaller scales. The main drivers for a smaller-scale PO production schemes include PO being used in many niche applications such as a fumigant and disinfectant for food,[7] a sterilizer for medical equipment,[8] as well as in forming modified food starch and alginate,[9] which do not necessarily require high volume and concentrations of PO. The need for the smaller-scale PO production routes is amplified by the very high toxicity of PO, making it not suitable for transportation and long-term storage.

Low-temperature plasma−liquid interaction (PLI) systems are an interesting new platform for chemical synthesis. These systems have been proposed as potentially useful for wastewater treatment,[10] medical applications,[11] and material and chemical synthesis/processing.[12−14] The interaction of plasma with liquids leads to the production of highly reactive oxidizing and reducing species, including free and solvated electrons, photons, ions, and radicals at the plasma−liquid interface.[15] Furthermore, compared to electro- and photo-catalytic systems, PLI can generate large fluxes of electrons with higher energies (up to 10 eV) which can activate a wide range of chemical transformations.[15,16] As these PLI systems only utilize gas-phase electrical discharge in contact with liquid (most often water) at ambient conditions, they are ideally suited for small-scale operations. Furthermore, the reliance on electrical energy as the primary energy source allows these processes to be easily coupled with renewable energy sources.[17]

Received: January 17, 2023
Revised: March 13, 2023
Accepted: March 14, 2023
Published: March 21, 2023

https://doi.org/10.1021/jacsau.3c00030
JACS Au 2023, 3, 997−1003

It has been demonstrated recently that H_2O_2 can be formed with relatively high efficiencies from water at plasma−water interfaces in PLI systems.[17−20] Herein, we designed a PLI system that uses this plasma-generated H_2O_2 to epoxidize C_3H_6 with very high PO selectivity in excess of 98%. The PLI process employed titanium silicate-1 (TS-1) catalysts dispersed in the water solution designed to contact the in situ produced H_2O_2 with dissolved C_3H_6. We emphasize that the process employs only water and C_3H_6 as reactants, and it does not require a gaseous mixture of O_2 and H_2 to generate H_2O_2.[21−23] We also discussed the impact of different plasma parameters on activity and selectivity for PO production. The presented findings provide us with a path toward on-demand production of PO from C_3H_6 and water, which can be useful in several niche applications.

Figure 1a shows the plasma reactor used in the studies (refer to Methods for experimental details). A pulsed, direct current

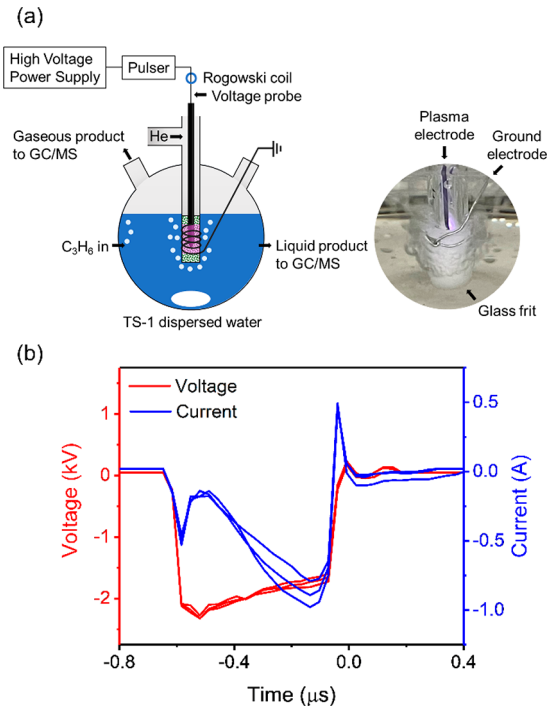

Figure 1. (a) Schematic of the plasma reactor setup (left) and photo of plasma discharge in water (right). (b) Initial voltage and current waveforms of a 0.5 μs pulsed discharge at a repetition rate of 1 kHz (He flow rate: 200 sccm). Measurements of three different pulses are shown. Solution condition: 4.5 mg/L TS-1 dispersed 30 mL deionized (DI) water constantly bubbled with 4 sccm of C_3H_6.

(DC) plasma discharge was generated by applying −2.4 kV to the tungsten needle plasma electrode (cathode) with a pulse width of 0.5 μs (frequency 1 kHz). The plasma electrode was inserted into the gas dispersion tube connected to a He gas inlet at a flow rate of 200 sccm. The aluminum wire surrounding the outside of the gas dispersion tube served as the ground electrode (anode) which makes direct electrical contact with the 30 mL of water (water anode). The tungsten needle and the aluminum wire were separated by a glass frit with a pore size of 4.5−5 μm. The inert He gas fed into the gas dispersion tube served as a purge gas through bubble formations in the liquid for removing dissolved oxygen and nitrogen species in water. Additionally, it served as a feed gas for plasma discharge. Therefore, the plasma-carrying He gas contacted the liquid by exiting the tube through a glass frit. This process leads to the plasma-encapsulating bubble formations within the liquid. It has been suggested to increase the efficiency of the mass transfer of the plasma-generated reactive species compared to typical microdischarge systems owing to the enhanced plasma−liquid interfacial area.[13,17,24]

Figure 1b shows the representative voltage and current waveforms measured at the plasma electrode at the initial stage of the discharge. The data are consistent with a filamentation of the atmospheric glow discharge which is expected at high discharge currents when a metal needle electrode is used.[25] The data show a classical feature of these types of plasma systems: a fast rise and fall of the applied voltage (~30 ns) that leads to an evolution of displacement current at both edges of the voltage rising and falling,[26] as well as an increasing discharge current. We note that these voltage and current waveforms are independent of the presence of both the C_3H_6 reactant and the TS-1 catalyst (Figure S1).

During the high-power density plasma discharge, free electrons are generated. These electrons can drive many different chemical transformations and generate numerous reactive species when interfaced with a liquid or liquid vapor at the plasma−liquid interface.[27] Figure 2 shows a sketch of a plasma-encapsulating bubble. We also show well-established chemical transformations, relevant for the H_2O_2 generation under these plasma conditions.[13,18] In plasma cathode/water anode systems, free plasma electrons can react with water vapors to form OH·. Depending on the energy of the free electrons (1−10 eV), the formation of the OH· proceeds via a water excitation reaction ($H_2O_{(g)} + e^-_{(g)} \rightarrow H_2O^*_{(g)} + e^-_{(g)}$; $H_2O^*_{(g)} + H_2O_{(g)} \rightarrow H\cdot_{(g)} + OH\cdot_{(g)} + H_2O_{(g)}$), a dissociative attachment of a free electron to water ($H_2O_{(g)} + e^-_{(g)} \rightarrow H^-_{(g)} + OH\cdot_{(g)}$), or via a direct ionization of water ($H_2O_{(g)} + e^-_{(g)} \rightarrow H\cdot_{(g)} + OH\cdot_{(g)} + e^-_{(g)}$).[13] It is generally agreed that $H_2O_{2(g)}$ is formed readily through the recombination of two $OH\cdot_{(g)}$.[28,29] The generated peroxide rapidly dissolves into the liquid phase ($H_2O_{2(g)} \rightarrow H_2O_{2(aq)}$). Alternatively, $H_2O_{2(aq)}$ can be also formed by the recombination of two dissolved $OH\cdot_{(aq)}$, which originates from the dissolution of the gas-phase $OH\cdot_{(g)}$ or dissociation of $H_2O_{(l)}$ at the plasma−water interface.[30] We show below that this dissolved H_2O_2 can selectively oxidize C_3H_6, resulting in the HPPO reaction (eq 1) to form PO. We note that without engineering the reactive environment to use it as an oxidizing agent, H_2O_2 molecules decompose to form H_2O and O_2 or are consumed by a dissolved electron, $e^-_{(aq)}$ ($e^-_{(aq)} + H_2O_{2(aq)} \rightarrow OH^-_{(aq)} + OH\cdot_{(aq)}$).

$$H_2O_{2(aq)} + C_3H_{6(aq)} \xrightarrow{\text{TS-1}} C_3H_6O_{(aq)} + H_2O_{(l)} \quad (1)$$

Propylene epoxidation was carried out in the reactor that employed spherical TS-1 nanoparticulate catalysts dispersed in DI water solution. C_3H_6 was constantly bubbled at a flow rate of 200 sccm through the water solution that was loaded with the TS-1 catalyst (Figure 1). The concentration of TS-1 in the water solution was 4.5 mg/mL, which corresponded to the maximum amount of TS-1 without noticeable solid precipitation. The spherical TS-1 nanoparticles, prepared by the hydrothermal method,[31,32] had an average diameter of around 200−300 nm based on scanning electron microscope (SEM) image analysis (Figure S2a). The X-ray diffraction (XRD) pattern showed a characteristic mordenite framework inverted (MFI)-type zeolite structure with the main diffraction features at 2θ = 7−9°, 23−25°, and 45° (Figure S2b).[31] A strong UV−

https://doi.org/10.1021/jacsau.3c00030
JACS Au 2023, 3, 997−1003

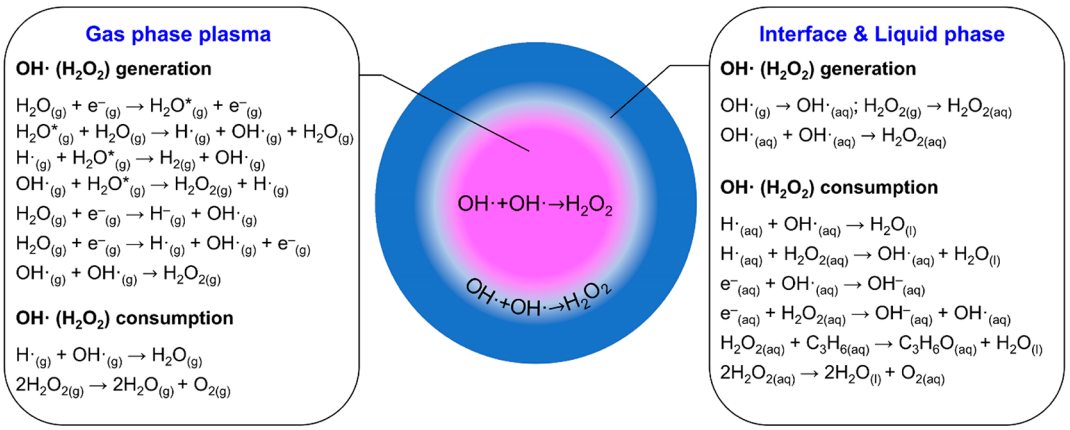

Figure 2. Reaction pathways of the H_2O_2 generation at the DC plasma cathode/water anode interface.[13,18] H_2O^* refers to the excited water.

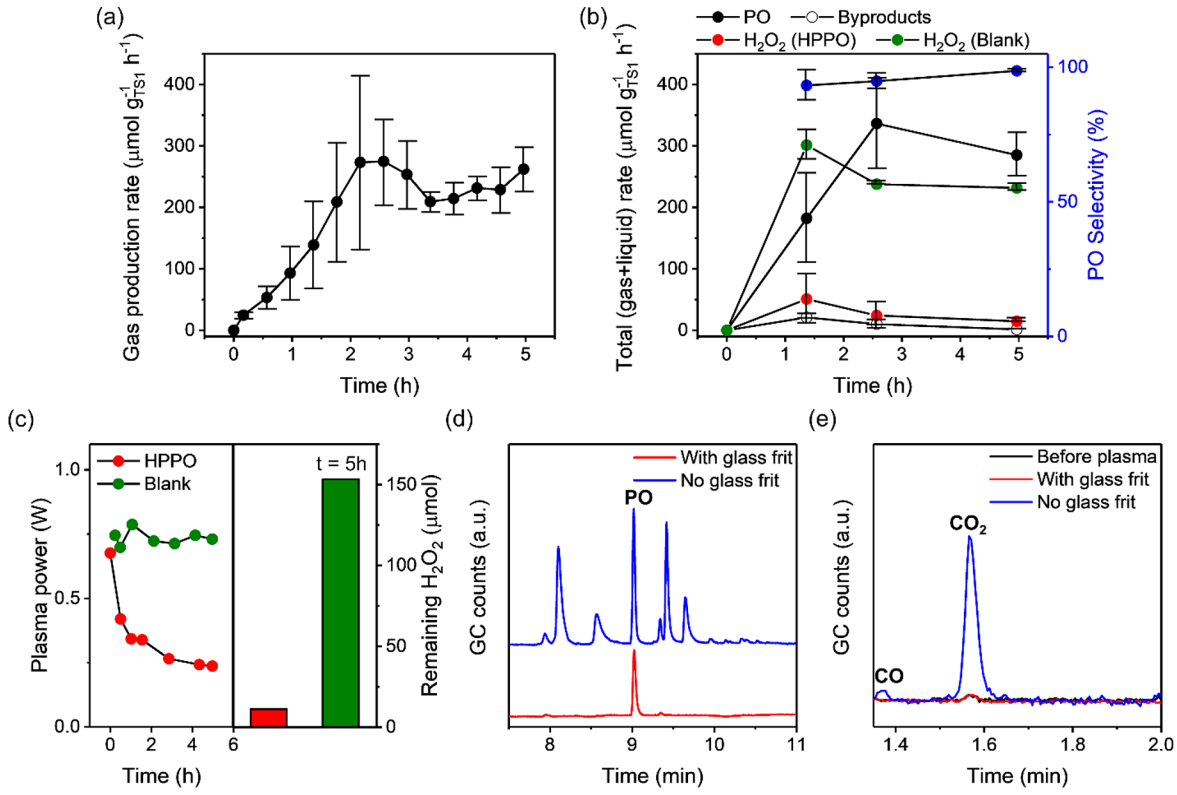

Figure 3. (a) Averaged production rates of gas-phase PO from four trials. (b) Production rates of total (gas + liquid) PO (black filled circle) and byproducts (black empty circle). The unreacted H_2O_2 (red) was also collected. H_2O_2 was also collected from the blank reaction (free of TS-1 and C_3H_6 flow) (green). PO selectivity is shown as blue circle. The data were obtained at t = 1.3, 2.5, and 5 h. (c) Left panel: average plasma power is plotted as a function of time, Right panel: remaining H_2O_2 detected after 5 h of reaction from blank (free of TS-1 and C_3H_6 flow) and HPPO samples. (d,e) Gaseous gas chromatography (GC) raw spectra measured with (red) and without (blue) glass frit at t = 5 h. A GC spectrum before plasma (black) is also plotted.

vis absorbance at <300 nm corresponds to the electron excitations at the isolated Ti sites in the TS-1 zeolite framework (Figure S2c).[31,33] Furthermore, a characteristic vibrational band at 960 cm^{-1} from the Fourier transform infrared (FTIR) spectroscopy measurements is due to the presence of Si−O−Ti bonds, which are characteristics of the TS-1 materials (Figure S2d).[31−33]

PO is generated in the liquid phase, while a majority of it is released into the gas phase. Data in Figure 3a show the averaged production rate (in μmol $g_{TS1}{}^{-1}$ h^{-1}) of PO detected in the gas phase as a function of time. The data were measured by collecting the products released into the gas phase (see Figure 1a) under a pulsed plasma condition every 24 min. Liquid samples were also collected at t = 1.3, 2.5, and 5 h, and the total product formation rate detected from both the gas and liquid phases is plotted in Figure 3b. We note that the considerable time required to reach the steady-state condition is most likely due to a relatively larger reactor size compared to the PO generation rate; i.e., the volumetric flux of plasma into the reactor is small compared to the volume of the liquid in the reactor. The data show that the PO selectivity is close to 100% with very slow production of byproducts which included 1-propanal, acetone, and isopropyl alcohol. These byproducts can be formed by either isomerization of PO on the TS-1

https://doi.org/10.1021/jacsau.3c00030
JACS Au 2023, 3, 997−1003

catalyst or by the reaction of C_3H_6 in an aqueous environment (Figure S4).[34] We also observed that the TS-1 catalysts exhibited a negligible change in morphology, crystallinity, and characteristic local structure after 5 h of operation (Figure S5).

To show that PO was formed through reactions of the plasma-generated H_2O_2 with C_3H_6 over TS-1 catalysts, we measured the amount of remaining H_2O_2 and produced PO with and without the TS-1 catalyst present in the solution (Table 1) after 5 h of reaction. Data in Figure S6 and Table 1

Table 1. Total Produced PO and Remaining H_2O_2 after the Five Hour HPPO and Additional Control Reactions

	produced PO (μmol)	remaining H_2O_2 (μmol)	PO selectivity (%)
HPPO	115	11	98.4
no TS-1 (with C_3H_6)	2	148	63.6
no C_3H_6 (with TS-1)	N/A	70	N/A
blank (No C_3H_6 and TS-1)	N/A	153	N/A

show that without TS-1 (no TS-1), a negligible amount of PO was produced and a significant amount of H_2O_2 remained in the solution. By comparing the data for no TS-1 and blank (no C_3H_6 and no TS-1) (Figure S6 and Table 1), it was found that the presence of C_3H_6 did not affect the rate of H_2O_2 consumption; i.e., without TS-1, H_2O_2 does not convert C_3H_6 to PO. Also, a negligible number of byproducts was generated (Figure S7). The data also show that as the TS-1 is introduced, the conversion of H_2O_2 reached 93% under steady-state conditions. Under these conditions, 81% of consumed H_2O_2 was utilized to form PO (eqs S4 and S5). We note that the calculated H_2O_2 selectivity toward the PO production represents a lower bound as the amount of produced H_2O_2 could be lower since the presence of TS-1 decreases the average plasma power with time, and as we found out that over time, the TS-1 catalyst was condensing and attaching to the ground electrode and increasing the resistance (Figure 3c and Figure S6c). This leads to a decrease in H_2O_2 production from the no C_3H_6 sample compared to the blank sample (Table 1). We also note that there was no obvious decomposition of H_2O_2 on TS-1 (Table S1). The high conversion of H_2O_2 (Figure 3b) suggests that at the stated conditions, the system operated in the regime in which the rate is limited by the rate of the in situ generation of H_2O_2.[32,35]

The data in Figure 3a,b and Table 1 show that under the given set of conditions, C_3H_6 reacts to form PO with very high selectivity. It is interesting to note that the selectivity to PO was significantly suppressed when the glass frit was removed (Figure 3d,e and Figure S8). Under these conditions, the rate of generation of deep oxidation products (i.e., CO_2) was enhanced compared to the rate of PO production. We note that the glass frit is essentially a high surface area, semipermeable silica membrane. We hypothesized that OH· reacted on silica surface which led to quenching of the radical[36] while allowing the relatively longer lived species like H_2O_2 to go through. It is well-established that OH· is a very strong oxidant that readily reacts with alkenes, forming deep oxidation products.[37]

Since the data above suggested that H_2O_2 is a limiting reagent in the current system, we probed some strategies that might improve the activity while maintaining the high selectivity of C_3H_6 epoxidation. For example, it has been shown that higher energy free electrons formed under an increased applied voltage are expected to result in higher OH· and H_2O_2 formation rates.[38] Similarly, increasing the flow rates of the plasma-carrying He gas should result in an increase in plasma−liquid interfacial area, enabling more efficient mass transfer of plasma-generated H_2O_2.[18] Led by these insights, we

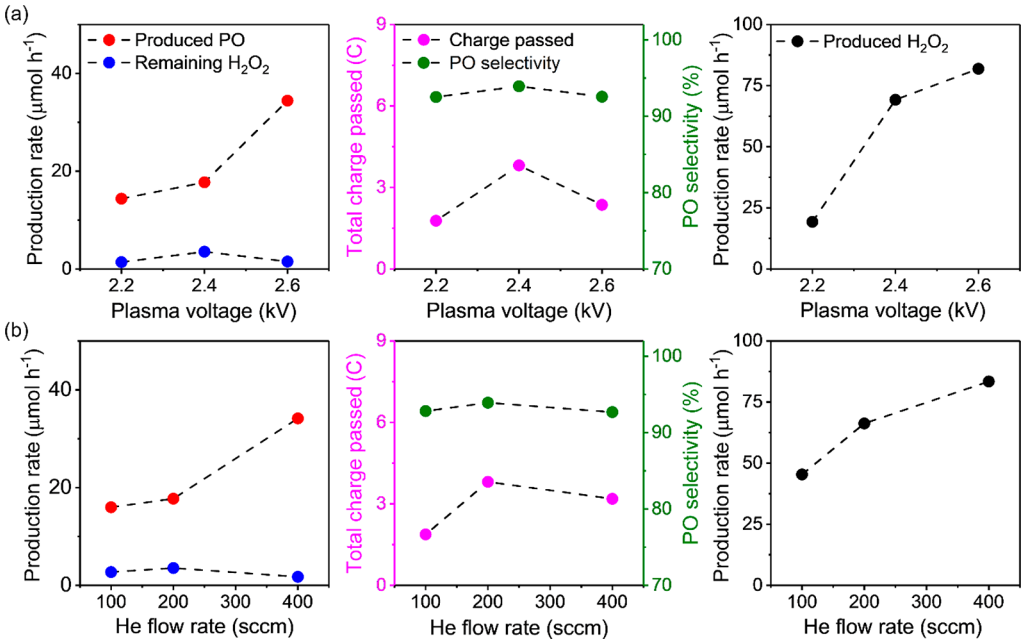

Figure 4. Effect of (a) plasma voltage and (b) He flow rate on the rates of total (gas + liquid) PO production (red) and remaining H_2O_2 (blue). PO selectivity (green) and total charge passed (pink) are also plotted. All data were obtained at the standard HPPO conditions with TS-1 catalyst and propylene. The rate of H_2O_2 production (black) was also measured for the blank solution free of TS-1 and C_3H_6 flow (right panels). Standard HPPO reaction conditions: solution (4.5 mg/L TS-1 dispersed 30 mL of DI water constantly bubbled with a 4 sccm of C_3H_6), plasma voltage (−2.4 kV), pulse width (0.5 μs with 1 kHz frequency), and He flow rate (200 sccm). Reaction time: 2.5 h.

https://doi.org/10.1021/jacsau.3c00030
JACS Au 2023, 3, 997−1003

analyzed the impact of plasma voltage and He flow rate on the rate of total PO production (detected from both the liquid and gas phases) and its selectivity (Figure 4). In each case, the reaction was operated for 2.5 h, i.e., long enough for the system to reach a steady state (Figure 3a). We note that this led to the PO selectivity of the standard reaction conditions to 94% (Figure 3b). The data in Figure 4a show that when the plasma voltage was increased from −2.2 to −2.6 kV, the PO production rate was also enhanced. Enhanced PO production was in line with the observed increase in the H_2O_2 production (Figure 4a right panel) under high applied voltage. We also observed improved PO production rates by increasing the flow rate from 100 to 400 sccm (Figure 4b). In both cases, high PO selectivity was maintained with negligible change in the total charge passed.

In summary, we designed a PLI catalytic process that uses water and C_3H_6 as reactants to form PO. We show that H_2O_2 generated through the interactions of water with plasma selectively oxidizes C_3H_6 to PO over TS-1 catalysts dispersed in the water solution. We measured a carbon-based selectivity of more than 98%. As the activity of the current plasma C_3H_6 epoxidation system is limited by the rate of H_2O_2 production, strategies to improve H_2O_2 production were also investigated.

METHODS

Plasma Reactor Setup

The plasma jet used in this study is similar to the one reported in the previous literature.[39] The plasma was generated at the tip of a tungsten needle electrode. A negative pulsed direct current (DC) voltage was applied to the tungsten needle by a DEI PVX-4110 high-voltage pulser. The tungsten needle was connected to a Spellman SL10N300 DC power supply through a 500 Ω resistor to limit the current in the discharge. The repetition frequency (was set to 1 kHz) and pulse width were set with a Tektronix AFG2021 Function generator. The needle electrode was inserted into a gas dispersion tube (fine frit with a pore size of 4.5−5 μm, Chemglass) in which the helium (He) working gas was supplied through Cole Palmer mass flow controllers at a flow rate of 200 sccm. The frit part of the gas dispersion tube was surrounded by a 0.5 mm diameter aluminum wire (Alfa Aesar) which was connected to earth ground. The entire glass frit part was then immersed in 30 mL of liquid in a custom-made round-bottom (RB) flask reactor. Plasma is generated between the tungsten needle (cathode) and the aluminum wire (anode), flows out through the glass frit and diffuses into the liquid, forming bubbles. The voltage (V) and current (I) profiles were monitored with a D-dot sensor and a Pearson 2877 Rogowski coil connected to a Tektronix DPO 2022B oscilloscope at the cathode side. The obtained voltage and current were used to calculate the average plasma power (P_{avg}).

$$P_{avg}(W) = \frac{1}{T}\int_0^T V(t)I(t)\mathrm{d}t \quad (2)$$

where T refers to the period (1000 μs) which refers to the amount of time between the start of one pulse and the start of the next.

Hydrogen Peroxide Propylene Epoxidation (HPPO)

The synthesized TS-1 was dispersed in DI water (4.5 mg/mL) by sonication and 30 mL of this solution was added to the RB flask reactor. The concentration of the TS-1 solution was chosen by dispersing the maximum amount of TS-1 without observing noticeable precipitation. The temperature of the entire reactor was set to 30 °C by immersing it in a temperature-controlled water bath. While 200 sccm of He gas was bubbled through the gas dispersion tube, propylene (C_3H_6) (99.9%, PurityPlus Gases) gas was fed into the TS-1 dispersed aqueous solution outside of the gas dispersion tube with a flow rate of 4 sccm to saturate the solution. The pressure of the inside of the gas dispersion tube was maintained at 17.2 psi, while that of the outside aqueous solution was maintained at 16.2 psi. This pressure difference allowed the He gas to flow out of the tube, preventing the backflow of the C_3H_6 gas. After 30 min of gas bubbling, the plasma discharge was initiated by applying −2.4 kV to the tungsten needle cathode with a pulse width of 0.5 μs (frequency 1 kHz). The applied voltage and current were recorded by an oscilloscope during the reaction. The solution was continuously stirred throughout the entire reaction process to increase the solution mixing and prevent TS-1 powder catalysts to precipitate at the bottom. The outlet gases were connected to the Agilent 7890B/5977A series gas chromatograph/mass selective detector (GC-MSD) system and were analyzed every 24 min. The liquid samples were first filtered through a 0.2 μm syringe filter (Whatman UNIFLO) and were manually injected into the GC-MSD system. Quantification of the products was based on the standard calibration curves obtained from the standard chemicals. To analyze the effect of different plasma parameters (i.e., plasma voltage and He flow rate) on PO production and selectivity, the 2.5 h HPPO reactions were repeated with changing parameters (plasma voltage: −2.2, −2.4, and −2.6 kV; He flow rate: 100, 200, and 400 sccm) while monitoring the voltage and current with the oscilloscope. The remaining H_2O_2 was also collected after the reaction.

ASSOCIATED CONTENT

Supporting Information

The Supporting Information is available free of charge at https://pubs.acs.org/doi/10.1021/jacsau.3c00030.

Experimental section; supplementary note; voltage and current waveforms in control reactions; SEM, XRD, UV−vis diffuse reflectance, and FTIR characterizations of TS-1; UV−vis absorption spectra of standard H_2O_2 solutions; proposed mechanism of byproducts production; TS-1 characterization before and after the reaction; product production, remaining H_2O_2, and average plasma power versus time; decomposition behavior of H_2O_2 with TS-1; liquid GC obtained with and without glass frit, and additional references (PDF)

AUTHOR INFORMATION

Corresponding Author

Suljo Linic − *Department of Chemical Engineering, University of Michigan, Ann Arbor, Michigan 48109, United States;* orcid.org/0000-0003-2153-6755; Email: linic@umich.edu

Authors

Dongho Lee − *Department of Chemical Engineering, University of Michigan, Ann Arbor, Michigan 48109, United States;* Present Address: Department of Chemistry, University of Ulsan, Ulsan 44776, Republic of Korea; orcid.org/0000-0001-8607-9976

https://doi.org/10.1021/jacsau.3c00030
JACS Au 2023, 3, 997−1003

Han-Ting Chen − *Department of Chemical Engineering, University of Michigan, Ann Arbor, Michigan 48109, United States;* orcid.org/0000-0002-6942-718X

Complete contact information is available at: https://pubs.acs.org/10.1021/jacsau.3c00030

Author Contributions

CRediT: **Dongho Lee** conceptualization, data curation, formal analysis, writing-original draft; **Han-Ting Chen** conceptualization, data curation, formal analysis, writing-original draft; **Suljo Linic** conceptualization, funding acquisition, project administration, writing-original draft.

Notes

The authors declare no competing financial interest.

■ ACKNOWLEDGMENTS

Research was primarily sponsored by the Army Research Office and was accomplished under Grant No. W911NF-20-1-0105. Secondary support on materials characterization was provided by the Office of Basic Energy Science, Division of Chemical Sciences (DE-SC0021008). The views and conclusions contained in this document are those of the authors and should not be interpreted as representing the official policies, either expressed or implied, of the Army Research Office or the U.S. Government. The U.S. Government is authorized to reproduce and distribute reprints for Government purposes notwithstanding any copyright notation herein. The authors thank Dr. Jingkai Jiang and Prof. Peter Bruggeman (University of Minnesota Twin Cities) for assistance with the plasma jet.

■ REFERENCES

(1) Marimuthu, A.; Zhang, J. W.; Linic, S. Tuning Selectivity in Propylene Epoxidation by Plasmon Mediated Photo-Switching of Cu Oxidation State. *Science* **2013**, *339*, 1590−1593.

(2) Russo, V.; Tesser, R.; Santacesaria, E.; Di Serio, M. Chemical and Technical Aspects of Propene Oxide Production via Hydrogen Peroxide (HPPO Process). *Ind. Eng. Chem. Res.* **2013**, *52*, 1168−1178.

(3) Terzan, J.; Hus, M.; Likozar, B.; Djinovic, P. Propylene Epoxidation Using Molecular Oxygen over Copper- and Silver-Based Catalysts: A Review. *ACS Catal.* **2020**, *10*, 13415−13436.

(4) Christopher, P.; Linic, S. Shape- and Size-Specific Chemistry of Ag Nanostructures in Catalytic Ethylene Epoxidation. *ChemCatChem.* **2010**, *2*, 78−83.

(5) Christopher, P.; Linic, S. Engineering Selectivity in Heterogeneous Catalysis: Ag Nanowires as Selective Ethylene Epoxidation Catalysts. *J. Am. Chem. Soc.* **2008**, *130*, 11264−11265.

(6) Yang, S.; Verdaguer-Casadevall, A.; Arnarson, L.; Silvioli, L.; Colic, V.; Frydendal, R.; Rossmeisl, J.; Chorkendorff, I.; Stephens, I. E. L. Toward the Decentralized Electrochemical Production of H_2O_2: A Focus on the Catalysis. *ACS Catal.* **2018**, *8*, 4064−4081.

(7) Danyluk, M. D.; Uesugi, A. R.; Harris, L. J. Survival of Salmonella Enteritidis PT 30 on Inoculated Almonds after Commercial Fumigation with Propylene Oxide. *J. Food Prot.* **2005**, *68*, 1613−1622.

(8) Sato, H.; Kidaka, T.; Hori, M. Sterilization of Therapeutic Immunoadsorbents with Aqueous Propylene-Oxide Solution. *Int. J. Artif. Organs* **1985**, *8*, 109−114.

(9) *Propylene Oxide - Environmental Health Criteria 56*; Finland, 1985.

(10) Singh, R. K.; Fernando, S.; Baygi, S. F.; Multari, N.; Thagard, S. M.; Holsen, T. M. Breakdown Products from Perfluorinated Alkyl Substances (PFAS) Degradation in a Plasma-Based Water Treatment Process. *Environ. Sci. Technol.* **2019**, *53*, 2731−2738.

(11) Fridman, G.; Friedman, G.; Gutsol, A.; Shekhter, A. B.; Vasilets, V. N.; Fridman, A. Applied Plasma Medicine. *Plasma Process Polym.* **2008**, *5*, 503−533.

(12) Mariotti, D.; Patel, J.; Svrcek, V.; Maguire, P. Plasma-Liquid Interactions at Atmospheric Pressure for Nanomaterials Synthesis and Surface Engineering. *Plasma Process Polym.* **2012**, *9*, 1074−1085.

(13) Locke, B. R.; Shih, K. Y. Review of the Methods to Form Hydrogen Peroxide in Electrical Discharge Plasma with Liquid Water. *Plasma Sources Sci. Technol.* **2011**, *20*, 034006.

(14) Hawtof, R.; Ghosh, S.; Guarr, E.; Xu, C.; Mohan Sankaran, R.; Renner, J. N. Catalyst-Free, Highly Selective Synthesis of Ammonia from Nitrogen and Water by a Plasma Electrolytic System. *Sci. Adv.* **2019**, *5*, No. eaat5778.

(15) Bruggeman, P. J.; Frontiera, R. R.; Kortshagen, U. R.; Kushner, M. J.; Linic, S.; Schatz, G. C.; Andaraarachchi, H.; Exarhos, S.; Jones, L. O.; Mueller, C. M.; Rich, C. C.; Xu, C.; Yue, Y. F.; Zhang, Y. Plasma-Driven Solution Electrolysis. *J. Appl. Phys.* **2021**, *129*, 200902.

(16) Gopalakrishnan, R.; Kawamura, E.; Lichtenberg, A. J.; Lieberman, M. A.; Graves, D. B. Solvated Electrons at the Atmospheric Pressure Plasma-Water Anodic Interface. *J. Phys. D: Appl. Phys.* **2016**, *49*, 295205.

(17) Zhou, R. W.; Zhang, T. Q.; Zhou, R. S.; Wang, S.; Mei, D. H.; Mai-Prochnow, A.; Weerasinghe, J.; Fang, Z.; Ostrikov, K.; Cullen, P. J. Sustainable Plasma-Catalytic Bubbles for Hydrogen Peroxide Synthesis. *Green Chem.* **2021**, *23*, 2977−2985.

(18) Cameli, F.; Dimitrakellis, P.; Chen, T. Y.; Vlachos, D. G. Modular Plasma Microreactor for Intensified Hydrogen Peroxide Production. *ACS Sustain. Chem. Eng.* **2022**, *10*, 1829−1838.

(19) Takeuchi, N.; Ishibashi, N. Generation Mechanism of Hydrogen Peroxide in DC Plasma with a Liquid Electrode. *Plasma Sources Sci. Technol.* **2018**, *27*, 045010.

(20) Wang, H. H.; Wandell, R. J.; Tachibana, K.; Vorac, J.; Locke, B. R. The Influence of Liquid Conductivity on Electrical Breakdown and Hydrogen Peroxide Production in a Nanosecond Pulsed Plasma Discharge Generated in a Water-Film Plasma Reactor. *J. Phys. D: Appl. Phys.* **2019**, *52*, 075201.

(21) Zhao, J. L.; Zhou, J. C.; Su, J.; Guo, H. C.; Wang, X. S.; Gong, W. M. Propene Epoxidation with In-Site H_2O_2 Produced by H_2/O_2 Non-Equilibrium Plasma. *AIChE J.* **2007**, *53*, 3204−3209.

(22) Miao, C. L.; Zhu, Q. R.; Yi, Y. H.; Su, J.; He, N.; Liu, J. X.; Guo, H. C. Gas-Phase Epoxidation of Propylene with Hydrogen Peroxide Vapor: Effect of Modification with NaOH on TS-1 Titanosilicate Catalyst in the Presence of Tetra-propylammonium Bromide. *Ind. Eng. Chem. Res.* **2019**, *58*, 11739−11749.

(23) Su, J.; Zhou, J. C.; Liu, C. Y.; Wang, X. S.; Guo, H. C. Gas Phase Epoxidation of Propylene with TS-1 and In Situ H_2O_2 Produced by a H_2/O_2 Plasma. *Chinese J. Catal.* **2010**, *31*, 1195−1199.

(24) Hong, J.; Zhang, T.; Zhou, R.; Zhou, R.; Ostikov, K.; Rezaeimotlagh, A.; Cullen, P. J. Plasma Bubbles: a Route to Sustainable Chemistry. *AAPPS Bulletin* **2021**, *31*, 26.

(25) Walsh, J. L.; Bruggeman, P. Filamentation of Diffuse He-H_2O Atmospheric Pressure Glow Discharges in a Metal Pin-Water Electrode Geometry. *IEEE Trans. Plasma Sci.* **2011**, *39*, 2634−2635.

(26) Walsh, J. L.; Kong, M. G. Room-Temperature Atmospheric Argon Plasma Jet Sustained with Submicrosecond High-Voltage Pulses. *Appl. Phys. Lett.* **2007**, *91*, 221502.

(27) Bruggeman, P J; Kushner, M J; Locke, B R; Gardeniers, J G E; Graham, W G; Graves, D B; Hofman-Caris, R C H M; Maric, D; Reid, J P; Ceriani, E; Fernandez Rivas, D; Foster, J E; Garrick, S C; Gorbanev, Y; Hamaguchi, S; Iza, F; Jablonowski, H; Klimova, E; Kolb, J; Krcma, F; Lukes, P; Machala, Z; Marinov, I; Mariotti, D; Mededovic Thagard, S; Minakata, D; Neyts, E C; Pawlat, J; Petrovic, Z L.; Pflieger, R; Reuter, S; Schram, D C; Schroter, S; Shiraiwa, M; Tarabova, B; Tsai, P A; Verlet, J R R; von Woedtke, T; Wilson, K R; Yasui, K; Zvereva, G Plasma-Liquid Interactions: a Review and Roadmap. *Plasma Sources Sci. Technol.* **2016**, *25*, 053002.

(28) Winter, J; Tresp, H; Hammer, M U; Iseni, S; Kupsch, S; Schmidt-Bleker, A; Wende, K; Dunnbier, M; Masur, K; Weltmann, K.-D.; Reuter, S Tracking Plasma Generated H_2O_2 from Gas into Liquid Phase and Revealing its Dominant Impact on Human Skin Cells. *J. Phys. D: Appl. Phys.* **2014**, *47*, 285401.
(29) Keniley, S.; Uner, N. B.; Perez, E.; Sankaran, R. M.; Curreli, D. Multiphase Modeling of the DC Plasma-Water Interface: Application to Hydrogen Peroxide Generation with Experimental Validation. *Plasma Sources Sci. Technol.* **2022**, *31*, 075001.
(30) Chen, Z. Y.; Liu, D. X.; Chen, C.; Xu, D. H.; Liu, Z. J.; Xia, W. J.; Rong, M. Z.; Kong, M. G. Analysis of the Production Mechanism of H_2O_2 in Water Treated by Helium DC Plasma Jets. *J. Phys. D: Appl. Phys.* **2018**, *51*, 325201.
(31) Khomane, R. B.; Kulkarni, B. D.; Paraskar, A.; Sainkar, S. R. Synthesis, Characterization and Catalytic Performance of Titanium Silicalite-1 Prepared in Micellar Media. *Mater. Chem. Phys.* **2002**, *76*, 99−103.
(32) Ko, M.; Kim, Y.; Woo, J.; Lee, B.; Mehrotra, R.; Sharma, P.; Kim, J.; Hwang, S. W.; Jeong, H. Y.; Lim, H.; Joo, S. H.; Jang, J. W.; Kwak, J. H. Direct Propylene Epoxidation with Oxygen using a Photo-Electro-Heterogeneous Catalytic System. *Nat. Catal.* **2022**, *5*, 37−44.
(33) Gordon, C. P.; Engler, H.; Tragl, A. S.; Plodinec, M.; Lunkenbein, T.; Berkessel, A.; Teles, J. H.; Parvulescu, A. N.; Coperet, C. Efficient Epoxidation over Dinuclear Sites in Titanium Silicalite-1. *Nature* **2020**, *586*, 708−713.
(34) Imanaka, T.; Okamoto, Y.; Teranishi, S. Isomerization of Propylene Oxide on Metal Phosphate Catalysts. *Bull. Chem. Soc. Jpn.* **1972**, *45*, 1353−1357.
(35) Delgado, H. E.; Brown, G. H.; Bartels, D. M.; Rumbach, P.; Go, D. B. The Scaling of Kinetic and Transport Behaviors in the Solution-Phase Chemistry of a Plasma-Liquid Interface. *J. Appl. Phys.* **2021**, *129*, 083303.
(36) Suh, M.; Bagus, P. S.; Pak, S.; Rosynek, M. P.; Lunsford, J. H. Reactions of Hydroxyl Radicals on Titania, Silica, Alumina, and Gold Surfaces. *J. Phys. Chem. B* **2000**, *104*, 2736−2742.
(37) Daranlot, J.; Bergeat, A.; Caralp, F.; Caubet, P.; Costes, M.; Forst, W.; Loison, J. C.; Hickson, K. M. Gas-Phase Kinetics of Hydroxyl Radical Reactions with Alkenes: Experiment and Theory. *ChemPhysChem* **2010**, *11*, 4002−4010.
(38) Yue, Y. F.; Exarhos, S.; Nam, J.; Lee, D.; Linic, S.; Bruggeman, P. J. Quantification of Plasma Produced OH and Electron Fluxes at the Liquid Anode and Their Role in Plasma Driven Solution Electrochemistry. *Plasma Sources Sci. Technol.* **2022**, *31*, 125008.
(39) Yue, Y. F.; Kondeti, V. S. S. K.; Sadeghi, N.; Bruggeman, P. J. Plasma Dynamics, Instabilities and OH Generation in a Pulsed Atmospheric Pressure Plasma with Liquid Cathode: a Diagnostic Study. *Plasma Sources Sci. Technol.* **2022**, *31*, 025008.

https://doi.org/10.1021/jacsau.3c00030
JACS Au 2023, 3, 997−1003